Available online at www.sciencedirect.com
ScienceDirect
Ceramics International 36 (2010) 567–575
CERAMICS INTERNATIONAL
www.elsevier.com/locate/ceramint

Evolution of microstructure, mineralogy and properties during firing of clay-based ceramics with borates

A. Christogerou [a], T. Kavas [b], Y. Pontikes [a], C. Rathossi [c], G.N. Angelopoulos [a,*]

[a] Laboratory of Materials and Metallurgy, Department of Chemical Engineering, University of Patras, 26500 Rio, Greece
[b] Department of Material Science and Engineering, Afyon Kocatepe University, Afyonkarahisar, Turkey
[c] Section of Earth Materials, Department of Geology, University of Patras, 26500 Rio, Greece

Received 27 July 2009; received in revised form 4 September 2009; accepted 20 September 2009
Available online 29 October 2009

Abstract

The effect of sieve boron waste (SBW) and borate-containing Evansite® on the thermal behaviour, microstructure and properties of a clay-based body was investigated. SBW and Evansite® were introduced in quantities that correspond to 0.6 wt.% B_2O_3 addition in the dry body for both cases. Cylindrical samples were extruded and fired at three different peak temperatures 900, 950 and 1000 °C. The reference body, R, and the body with SBW, RB, demonstrate a comparable dilatometric behaviour whereas the densification for the body with Evansite®, RV, initiated 50 °C approximately lower and resulted in higher firing shrinkage. After firing at 900 °C, the physico-mechanical properties as well as the microstructure are comparable. Nonetheless, åkermanite is formed in RB, whereas hercynite and mullite, the latter at 1000 °C, are formed in RV. For firing at 1000 °C, the role of borates is intensified. Water absorption is reduced by 16.1% and 18.0%, whereas bending strength increased by 27.6% and 40.8%, for RB and RV respectively, compared to the reference formulation. This is attributed predominantly to the enhanced vitrification that took place in the boron-containing bodies.

Keywords: A. Extrusion; A. Firing; B. Microstructure-final; D. Traditional ceramics; Borates

1. Introduction

The largest reserves of borates occur in West Turkey, with a worldwide share of 72% (851Mt) in terms of B_2O_3 content, and are controlled by the national mining enterprise Eti Maden Works [1,2]. In 2008 the production amounted to 2.25 million tons, with 4.1 million tons being the world's total production without the US share included [3]. The principal sedimentary borate ore minerals are borax decahydrate ($Na_2O{\cdot}2B_2O_3{\cdot}10H_2O$), ulexite ($Na_2O{\cdot}2CaO{\cdot}5B_2O_3{\cdot}16H_2O$) and colemanite ($2CaO{\cdot}3B_2O_3{\cdot}5H_2O$) which are refined into pure chemical compounds [4]. During this process large quantities (~400.000 tons/y) of different types of solid boron wastes are formed and rejected in tailing dams [5]. It is expected that over the next several years the demand for borates will increase [3] (although projections may need revisions in view of the financial crisis). As a consequence, the amount of boron wastes will increase too.

Utilisation of boron-containing wastes in the heavy clay industry may improve the quality of the final products and simultaneously diminish the disposal and leaching problems. According to Uslu and Arol [6], addition of up to 30 wt.% of clay containing tailings in a clay mixture suitable for red brick production enhances the formation of glassy phase and improves the overall brick quality. Higher additions reduce the compressive strength and deteriorate the surface of the bodies. Kavas [7] reports that introducing clay and fine boron wastes up to 15 wt.% in mixtures with Bayer's process red mud, results in the formation of glassy phase improving the mechanical properties of the fired bodies. Kurama et al. [8], studied a mixture consisting of dewatered sieve waste, ball clay and sanitaryware waste for the production of a terracotta floor tile body. It was found, also in this case, that the addition of BW promotes vitrification. The authors ascribe the improved physical and mechanical properties apart from the presence of boron to the high content of alkaline-earth oxides in the

* Corresponding author. Tel.: +30 2610969530; fax: +30 2610990917.
E-mail address: angel@chemeng.upatras.gr (G.N. Angelopoulos).

0272-8842/$36.00
doi:10.1016/j.ceramint.2009.09.039

Table 1
Chemical composition, in wt.%, of R and SBW.

	SiO_2	Al_2O_3	CaO	Fe_2O_3	MgO	K_2O	Na_2O	B_2O_3	L.O.I.
R	66.89	14.36	0.91	6.91	1.94	1.63	1.12	–	6.24
SBW	19.64	0.77	8.29	0.28	9.51	0.66	12.20	20.12	28.53

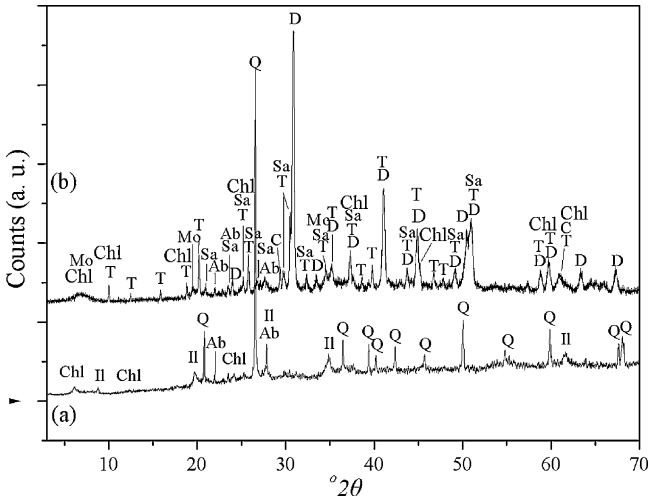

Fig. 1. XRD patterns of the raw materials (a) R and (b) SBW. *Abbreviations*—Qtz: quartz, Ab: albite, Sa: sanidine, Tin: tincalconite, D: dolomite, Cc: calcite, Ill: illite, Chl: chlorite, Mo: montorillonite.

boron waste that decrease the viscosity of the developed liquid phase. In a different work, Kurama et al. [9], investigate the same boron waste (addition up to 2 wt.%) as a partial substitution for Na-feldspar in the field of commercial wall tile production. Waste addition in controlled rates improved the vitrification and simultaneously enhanced the technological properties of the fired samples. The results indicate that this boron waste can be used as a ''co-flux'' in the wall tile formulation. Elbeyli et al. [10] studied the utilisation of a treated borax waste (mainly consisting of clay minerals) for brick production. Samples with different amounts of borax waste (addition up to 30 wt.%) were dry pressed and fired. It was demonstrated that the physical properties of the final bodies were negatively affected as the amount of borax waste increased. Nevertheless, the optimum waste ratio according to the authors accounts to 10 wt.%, which gives compressive strength values higher than the reference formulation. Olgun et al. [11] tested the effect of coal fly ash and borax solid waste on the properties of wall tiles. Potassium feldspar was replaced by fly ash in the range of 2–10 wt.%, while the boron waste remained at fixed quantities, 2 wt.% and 5 wt.% respectively. It was observed that the firing strength of the tiles containing boron waste is higher than that of the reference tile and the one containing fly ash. Moreover, addition of up to 6 wt.% boron waste as potassium feldspar replacement improved the strength values. More recently, Christogerou et al. [12], report on the addition of 5 wt.% (0.6 wt.% B_2O_3) and 15 wt.% (1.9 wt.% B_2O_3) of a sieve boron waste in a dry pressed clay body mixture. The addition of 5 wt.% resulted in higher bending strength, whereas the mixture with 15 wt.% deformed at high firing temperatures due to enhanced liquid phase formation.

A challenging issue on the use of borates in the heavy clay industry concerns the water solubility of borates. Tests with borax ($Na_2B_4O_7{\cdot}10H_2O$) and boric acid (H_3BO_3) in clay bodies showed migration of boron to the clay surface as the water is expelled during drying [13]. Consequently on firing, the surface is prone to viscous phase formation, creating problems in the production and the quality of the end-product. Due to the awareness of boron solubility, the various studies found in the open literature concerning boron waste utilisation in brick and tile production have in common that the formation of the samples is based on dry pressing.

To counter the solubility issues of borates, researchers developed and patented [14] a sugar-based microcrystalline sodium pentaborate suspension that was commercially available under the name Evansite® by Borax®. Austerberry and Stubbs found that addition of 1–2% Evansite® in a clay body mixture [13] decreases the water absorption whereas increases the compressive strength and the abrasion resistance. Therefore, a reduction of firing temperature by 50 °C approximately is feasible. This approach permitted the use of borates in processes that involved plastic forming, such as extrusion.

In the present work, sieve boron waste or Evansite® are introduced in a clay-based mixture aiming to investigate their behaviour during a processing cycle comparable with that followed in the heavy clay industry.

2. Experimental procedure

The raw materials used were clay body mixture, R, industrially used in W. Greece for the production of reddish roofing tiles, and SBW, a boron waste supplied from Etibor Co. Kirka Borax plant in Turkey. This waste derives from the first treatment of the boron ore, which includes the steps of crushing,

Table 2
Semi-quantitative, wt.%, mineralogical composition of the raw materials. *Abbreviations*—Qtz: quartz, Ab: albite, Sa: sanidine, Tin: tincalconite, D: dolomite, Cc: calcite, Ill: illite, Chl: chlorite, Mo: montorillonite and n.d.: not detected.

	Qtz	Ab	Sa	Tin	D	Cc	Ill	Chl	Mo
R	50.1	16.4	6.9	n.d.	n.d.	n.d.	19.9	6.7	n.d.
SBW	n.d.	14.9	11.1	29.3	27.5	6.2	n.d.	6.2	4.8

washing and sieving, and results in the production of the concentrate ore. Evansite® was a commercially available suspension containing microcrystalline sodium pentaborate developed by Borax®. The chemical composition of R and SBW was determined by inductively coupled plasma optical emission spectrometry (ICP-OES Optima 3200 XL, PerkinElmer). The crystalline phases of the raw materials were determined by X-ray diffraction analysis (D8 Advance, Bruker-AXS). Qualitative analysis was performed by the DIFFRACplus EVA® software (Bruker-AXS) based on the ICDD Powder Diffraction File. The mineral phases were quantified using a Rietveld-based quantification routine with the TOPAS® software (Bruker-AXS). The routine is based on the calculation of a single mineral-phase pattern and the refinement of the pattern using a non-linear least squares routine [15]. A number of corrections, including among others the instrument's geometry, background, sample displacement, detector type, mass absorption coefficients of the refined phases and the preferred orientation of certain *h k l* planes were applied in order to achieve the optimum pattern fitting. The amorphous phase was calculated by the determination of degree of crystallinity.

For the preparation of the bodies, the raw materials were milled at a particle size <1 mm. SBW and Evansite® were introduced in quantities that correspond to 0.6 wt.% B_2O_3 addition as per dry body mixture, for both cases. The powders were mixed in an arm mixer and subsequently water was added. For the mixture with SBW, water addition was approximately 28 wt.%, whereas for the mixture with Evansite®, 23 wt.% water was introduced; along with the pre-calculated amount of Evansite® suspension the water content also in this case amounts to a total of 28 wt.%. The so-obtained mixtures with SBW and Evansite® were labelled RB and RV respectively.

The relatively small content of SBW (and B_2O_3) introduced in the bodies was due to a previous study [12], where a higher amount of SBW (15–1.9 wt.% B_2O_3) resulted in the deformation of the dry-pressed samples when fired >900 °C. Nonetheless, a second mixture, RB2, was also prepared with 10 wt.% SBW (1.9 wt.% B_2O_3) added to the dry clay mixture. The goal was to make more easily discernible the boron migration and its effect on drying/firing.

The plastic mixtures were kept 24 h closed in plastic bags for maturation. A vacuum pug mill (75 mm, mk2, Venco) was used for the extrusion of cylindrical samples, dia = 25 mm and *l* = 120 mm. The bodies in the complementary study with 10 wt.% SBW were shaped by hand. The green samples were left at room temperature for 24 h and then dried in a drying oven at 110 °C till constant weight was attained. Firing was performed in a laboratory muffle furnace at three peak temperatures: 900, 950 and 1000 °C, with 4 h soaking time. The specimens were cooled to room temperature inside the furnace.

For the fired ceramics, apparent porosity, water absorption and bulk density were determined according to ISO standard [16]. Bending strength was determined using a testing machine (DTM, Dillon) equipped with a three point bending fixture. Roller span was regulated at two-thirds of the sample length and crosshead speed was 1.5 mm min^{-1}. The crystalline phases of the fired samples were determined by XRD, as mentioned above, on pulverised bodies. For the thermal analysis, thermogravimetry (TGA Q50, TA Instruments), differential thermal analysis (DTA, 402, Netzsch) and dilatometry (402ES, Netzsch) were performed. TGA and DTA analysis was performed in powdered samples <125 μm, in static air with a heating rate of 10 °C/min. The TGA/DTA results are supported by XRD analysis on SBW, after heating at 10 °C/min and extraction of the sample from the furnace at designated temperatures. Dilatometry was conducted in static air with a heating and cooling rate of 5 °C/min. The specimens were rods, dia = 3 mm and *l* = 25 mm. Observation of microstructures was performed by scanning electron microscopy, SEM (JSM-6300, Jeol) on gold coated, polished surfaces. For microchemical analyses, an energy dispersive X-ray spectrometer, EDS (LINK

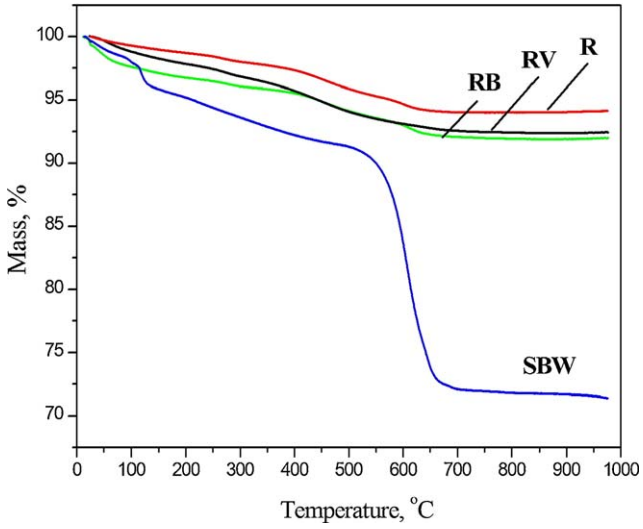

Fig. 2. TG curves for the raw materials R and SBW, and the mixtures RB and RV.

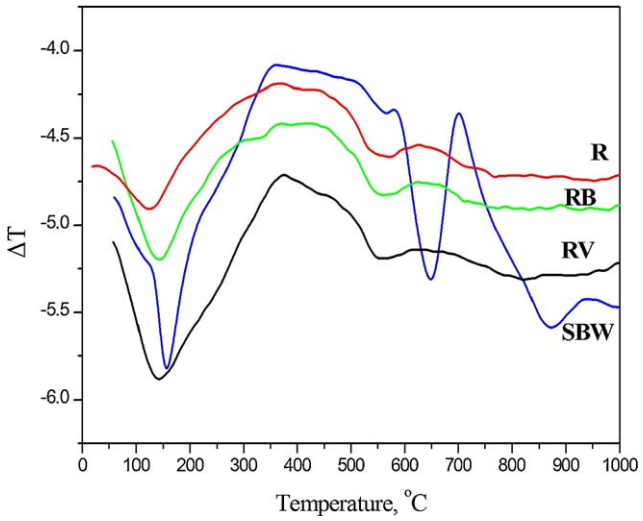

Fig. 3. DTA curves for the raw materials R and SBW, and the mixtures RB and RV.

PentaFET 6699, Oxford Instruments) was employed. The default standards of LINK ISIS have been used.

3. Results and discussion

3.1. Raw materials

The chemical analysis of the raw materials is reported in Table 1. The analysis of the clay body, R, reveals high levels of silica, the absence practically of calcium oxide and low levels of magnesium oxide. Contents of alumina and of iron oxide are 14.4 wt.% and 6.9 wt.% approximately. Those of alkaline oxides amount to 2.8 wt.% approximately. SBW has considerable high levels of boron and sodium that are expected to function as fluxing oxides. Alkaline earth oxides are also at high levels and are expected to contribute in the neomineralisation during firing [17]. Silica and alumina that act as network formers are 19.6 wt.% and less than 1 wt.% respectively. The high loss on ignition, 28.5 wt.% approximately, is expected to result in pore formation during firing, as seen also in other cases [12]. For Evansite®, the boron oxide content is 18% according to the manufacturer. The loss on ignition at 1000 °C was measured 48 wt.% approximately.

XRD patterns of the raw materials, R and SBW, are shown in Fig. 1, whereas the results for the semi-quantitative mineralogical analysis are presented in Table 2. For the clay body mixture, R, the identified phases are quartz SiO_2, albite $NaAlSi_3O_8$, sanidine $KAlSi_3O_8$, illite/muscovite $K_2Al_4[(Si_6Al_2)O_{20}](OH)_4$ and clinochlore $(Mg, Fe^{2+})_{10}Al_2[(Si_6Al_2)O_{20}](OH)_{16}$. This mixture can be considered as an illite-rich, non-calcareous sediment. For SBW, tincalconite $Na_2B_4O_7{\cdot}5H_2O$, dolomite $CaMg(CO_3)_2$ and albite $NaAlSi_3O_8$ are the main crystalline phases, at 29.3 wt.%, 27.5 wt.% and 14.9 wt.% respectively. In lower amounts, sanidine $KAlSi_3O_8$, calcite $CaCO_3$, chlorite $(Mg, Fe^{2+})_{10}Al_2[(Si_6Al_2)O_{20}](OH)_{16}$ and montmorillonite $(1/2Ca,Na)_{0.7}(Al, Mg, Fe)_4[(Si,Al)_8O_{20}](OH)_4\ nH_2O$ are also present.

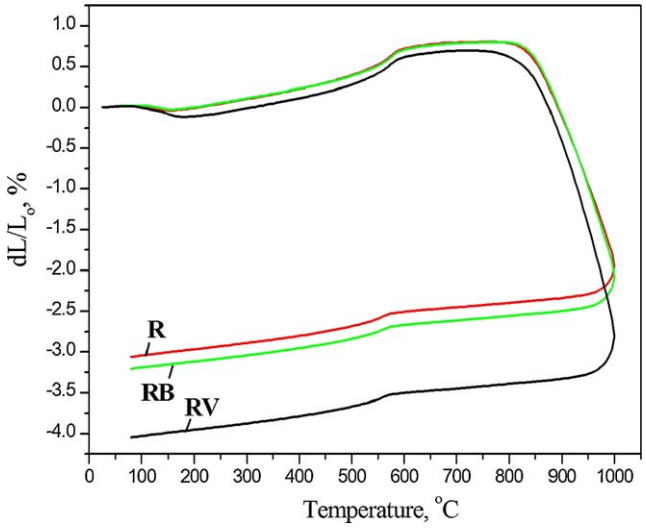

Fig. 4. Dilatometry curves for R, RB and RV.

3.2. Drying and firing behaviour

No visible salts were observed on the surface of the samples after drying at 110 °C. That applies for RB2 as well, although in this case, as will be discussed in Section 3.4, boron diffusion is discernible. The reduced mobility of borates, apart from the low

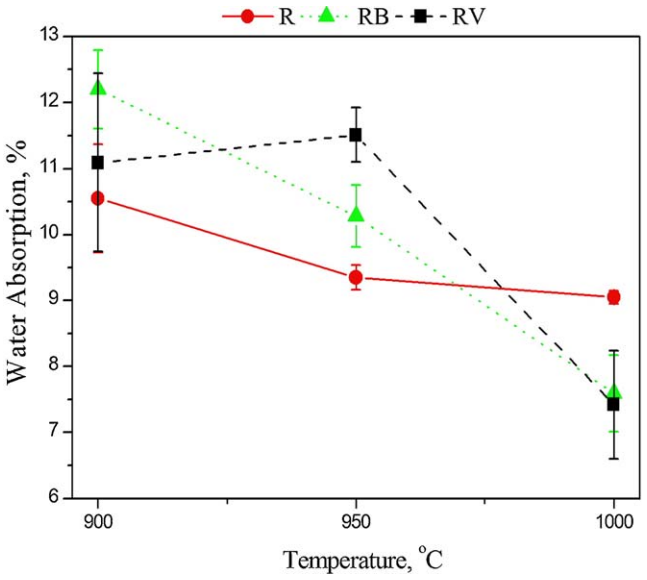

Fig. 5. Water absorption as a function of firing temperature for all tested samples.

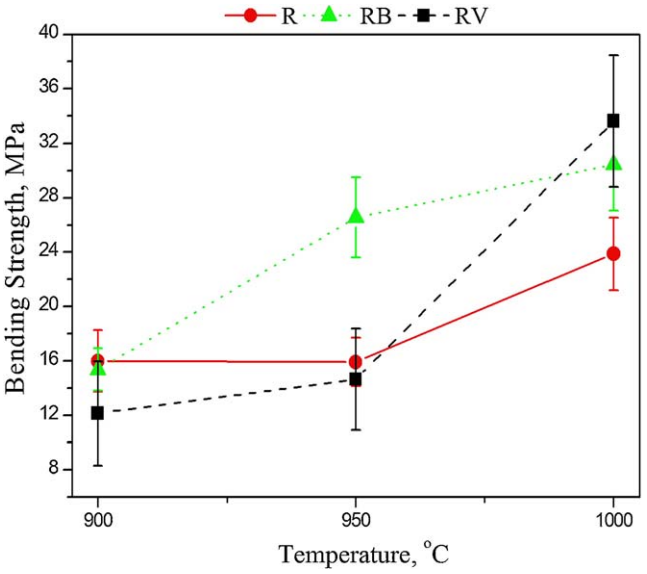

Fig. 6. Bending strength as a function of firing temperature for all tested samples.

Table 3
Moh's scale hardness of fired ceramics.

Firing temperature (°C)	R	RB	RV
900	7–8	8–9	8
950	7–8	9	8–9
1000	9	9	9

Table 4
Quantitative, wt.%, mineralogical composition of the fired samples at the three temperatures. *Abbreviations*—Qtz: quartz, Ab: albite, Sa: sanidine, He: hematite, Hc: hercynite, Åk: åkermanite, Mul: mullite, Mi: illite/muscovite and n.d: not detected.

	Temperature (°C)	Qtz	Ab	Sa	He	Hc	Åk	Mull	Mica	Amorphous	GOP
R	900	50.6(5)	12.7(7)	7.7(4)	5.4(3)	n.d.	n.d.	n.d.	4.6(7)	19.3	1.51
R	950	50.2(3)	12.1(7)	8.6(5)	6.5(2)	n.d.	n.d.	n.d.	n.d.	22.7	1.46
R	1000	48.9(2)	11.2(6)	6.8(4)	6.7(2)	n.d.	n.d.	n.d.	n.d.	26.4	1.49
RB	900	48.4(1)	10.6(8)	7.1(8)	5.9(3)	n.d.	1.3(5)	n.d.	4.0(7)	22.7	1.47
RB	950	47.2(1)	9.7(8)	8.9(3)	6.5(3)	n.d.	3.3(4)	n.d.	n.d.	24.3	1.38
RB	1000	45.5(3)	8.5(8)	5.9(5)	6.7(3)	n.d.	4.8(5)	n.d.	n.d.	28.7	1.49
RV	900	50.0(5)	10.7(6)	8.1(4)	6.0(3)	1.8(6)	n.d.	n.d.	4.4(7)	18.9	1.37
RV	950	48.9(5)	7.6(3)	6.5(6)	6.2(3)	2.1(3)	n.d.	n.d.	n.d.	28.8	1.38
RV	1000	40.3(1)	5.4(6)	4.6(5)	6.5(3)	3.1(3)	n.d.	2.8(4)	n.d.	37.2	1.36

percentage added, is attributed to a number of reasons: (a) the solubility of tincalconite is rather low; at 40 °C, is less than 12 wt.% in $Na_2B_4O_7$ [18]. Since the extrusion and first days of drying took place at room temperature (i.e. 22–25 °C) the solubility is expected to be even lower. (b) Only a fraction of the tincalconite in solution will migrate to the surface as this depends on the permeability (i.e. pores' size distribution, pores' shape, pores' connectivity, etc.) of the body. Indeed, it has been experimentally observed in the case of hand pelletising for lightweight aggregate production with boron wastes [19] that the results on surface salts depend on the exercised force by the operator. This is attributed to the different particle packing. To this extent, the results between RB and RB2 are not comparable as the latter samples have been shaped by hand.

The TGA and DTA analysis for the raw materials, R and SBW, as well as for the mixtures, RB and RV, is presented in Figs. 2 and 3, respectively. In the case of R, the overall weight loss is about 6 wt.% and is mainly due to dehydroxylation of the clay minerals. SBW has three characteristic steps of weight loss, Fig. 2. In the first step, up to 135 °C, the endothermic, Fig. 3, dehydration of tincalconite takes place. At 550 °C approximately, the dehydroxylation of tincalconite to anhydrous borax, $Na_2B_4O_7$, has been completed, in line with the accompanied weight loss, Fig. 2. In fact, the thermal behaviour of tincalconite resembles that of chemically pure borax $Na_2B_4O_7{\cdot}10H_2O$ [20,21]. Dolomite and calcite, originally present in SBW, start to dissociate at 530 °C approximately, as indicated by the weight loss, Fig. 2, and the strong endothermic peak, Fig. 3. This is an interesting result, as the dissociation starts at an early temperature, but in line with findings reported elsewhere [8]. It could be attributed either to the particle size of calcite and dolomite and/or to a catalytic effect [22] by the other constituents of the mixture. At 700 °C, the process is completed and there is subsequently minimal weight loss up to the final temperature. The weight loss between 530 and 700 °C is 18.7 wt.% which is in close agreement with the calculated loss due to CO_2 emission, based on the semi-quantitative analysis of Table 2. Moreover, the XRD pattern of SBW heated at 10 °C/min up to 750 °C and quenched at room temperature verify the absence of carbonates. The sample is composed of clinokurchatovite $Ca(Mg)B_2O_5$, augite $Ca(Mg,Fe,Al)(Si,Al)_2O_6$, sanidine $(K,Na)(Si_3Al)O_8$, albite $NaAlSi_3O_8$ and nepheline $NaAlSiO_4$.

The overall weight loss for SBW is approximately 28.5 wt.%. The TG curve of the mixture RB presents a small weight loss (approximately 2 wt.%) up to 70 °C. At 645 °C the weight loss for RB is completed and amounts to 8 wt.%. Comparable behaviour, in terms of both TGA and DTA, was observed for RV, with an overall weight loss of 7.5 wt.%.

The results of dilatometry are presented in Fig. 4. In general, R and RB demonstrate comparable behaviour whereas RV densifies at a lower temperature and has higher firing shrinkage. In the temperature interval 100–160 °C, RV shows higher shrinkage compared to R and RB. For the interval 200 to 500 °C, as well as 600 to 750 °C, all bodies present comparable thermal expansion coefficient. At 570 °C approximately, the transformation of α- to β-quartz, accompanied by volume expansion, is evident. The densification for RV begins at 760 °C, whereas for R and RB initiates at higher temperature, 810 °C. The overall shrinkage is 3.1%, 3.2% and 4.0% approximately for R, RB and RV respectively. The higher shrinkage of RV, in conjunction with the similar to RB weight loss during firing, Fig. 2, are indicative for reduced open porosity for RV compared to RB after firing at 1000 °C.

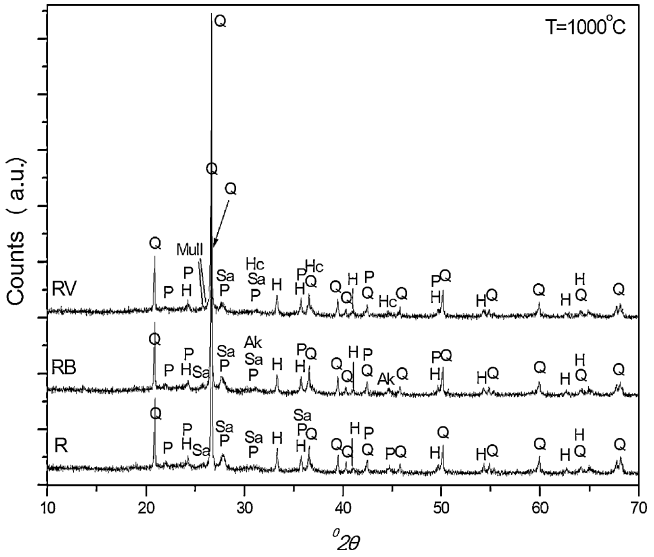

Fig. 7. XRD patterns of the samples R, RB and RV, fired at 1000 °C. *Abbreviations*—Q: quartz, P: plagioclase (albite), H: hematite, Sa: sanidine, Hc: hercynite, Åk: åkermanite, Mul: mullite.

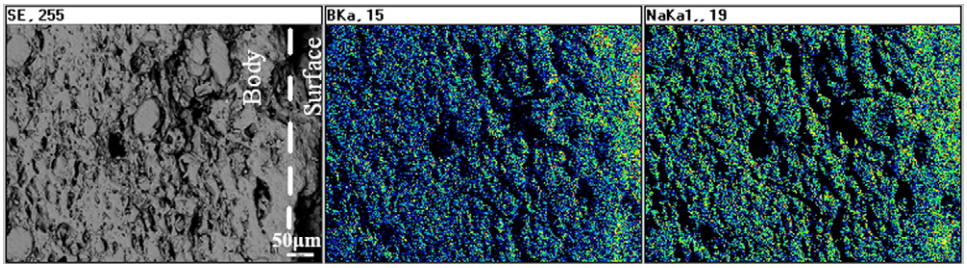

Fig. 8. Elemental mapping of polished cross section of RB2 after firing at 1000 °C. Dashed line marks approximately the surface of the sample. Left to right: Secondary electrons' image, B distribution, Na distribution.

3.3. Physico-mechanical properties

The results of water absorption are depicted in Fig. 5. It is observed that at lower firing temperatures, 900 °C, RB and RV show higher water absorption than R. Indeed, this is in line with the high weight loss recorded for RB and RV, Fig. 2. At 950 °C, both R and RB present lower water absorption compared to 900 °C; the values for RV do not diminish. Nevertheless, RB and RV still present higher water absorption than R. At 1000 °C, minor decrease is observed for R. On the contrary, RB and RV show a noticeable decrease and the obtained values are 7.6% and 7.4% respectively. Compared to the reference body fired at 1000 °C, water absorption is decreased by 16% and 18% for RB and RV respectively. The above results suggest that RB and RV become more reactive at $>$ 950 °C, which is in agreement with other works [12,13].

Fig. 6 presents the bending strength of the ceramics as a function of firing temperature. At 900 °C, all bodies demonstrate comparable values, with RV having the lowest strength compared to R and RB. Increasing the temperature at 950 °C, RB presents a notable increase to 26.6 MPa whereas R and RV undergo a slight increase to 15.9 MPa and 14.6 MPa

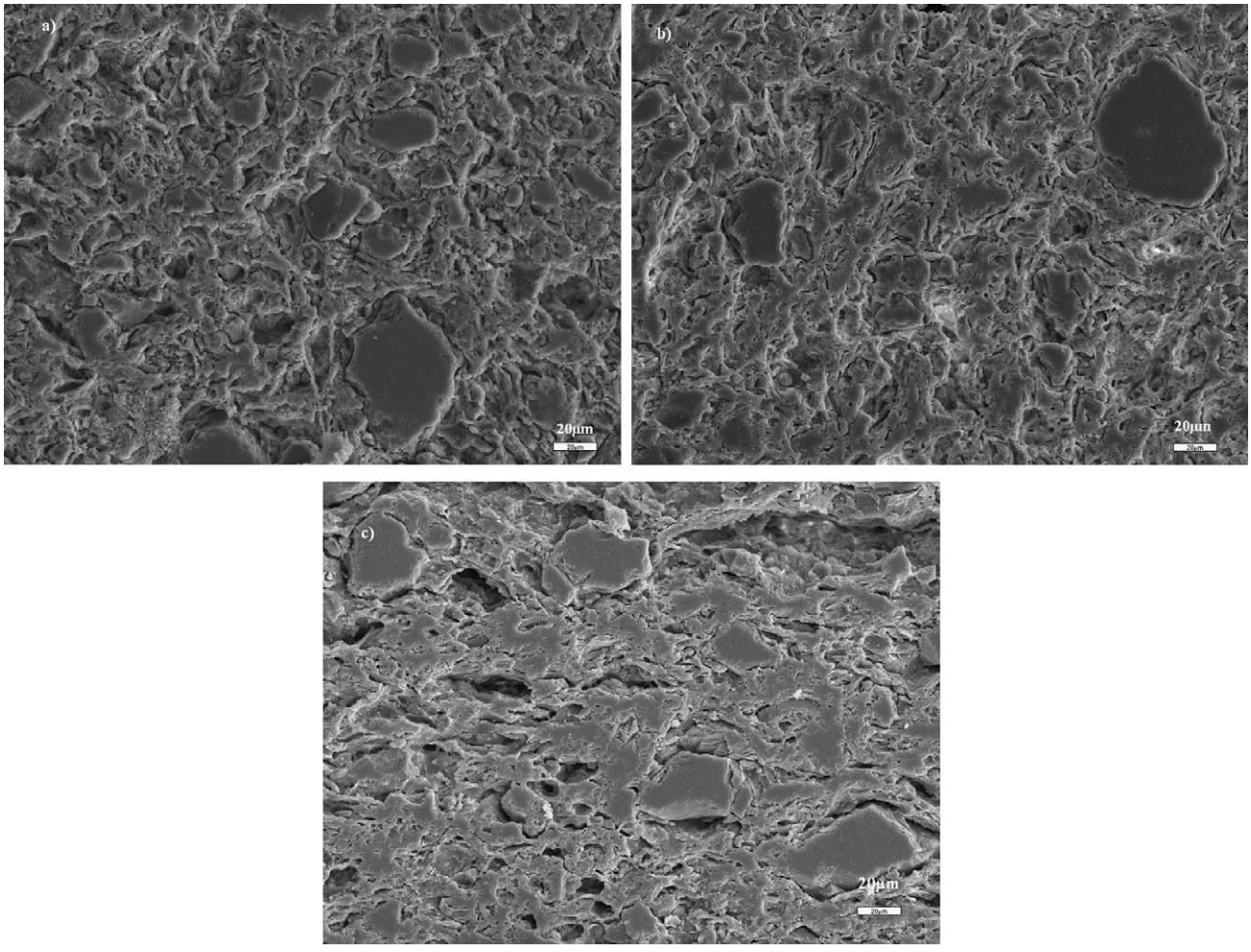

Fig. 9. Secondary electrons' images of polished surface of (a) R, (b) RB and (c) RV, fired at 900 °C.

respectively. For firing at 1000 °C, the bending strength of RV increases considerably to 33.6 MPa, whereas RB and R also increase to 30.7 MPa and 23.9 MPa respectively.

Table 3 shows the Mohs' hardness of the fired ceramics as a function of firing temperature. Addition of SBW into the clay mixture and firing at 900 °C leads to increased hardness, 8–9, compared to the reference samples, 7–8, and the one with Evansite, 8. Similar behaviour is observed at 950 °C, where the bodies with SBW presented higher hardness than R and RV. For firing at 1000 °C, all bodies show the same hardness.

3.4. Crystalline phases and microstructure

The mineralogical assemblage for R and RV is typical for a calcium-poor clay-based ceramic, Table 4. At 900 °C, the main phases identified by XRD for both samples are quartz, albite, sanidine, hematite, mica and amorphous; RV has in addition hercynite ($Fe^{2+}Al_2O_4$). The crystallisation of hercynite indicates that reducing conditions were created during the firing process [23], probably due to the combustion of organic matter in Evansite®. The formation of hematite is attributed to the iron released after the dehydroxylation of chlorite and illite minerals. In general, there are not significant variations in the crystalline composition between R and RV at this temperature.

As the firing temperature increases, mica disappears due to the complete breakdown of its structure. Quartz, albite and sanidine decrease, hematite remains practically stable whereas the amorphous content increases. For RV fired at 1000 °C, hercynite increases to 3.1 wt.% and mullite, most probably formed after the complete structural destruction of dehydroxylated mica [24], is the new mineral detected. From 950 to 1000 °C for RV, the percentage of quartz decreases drastically, from 48.9 wt.% to 40.3 wt.%, while the content of amorphous increases significantly, from 28.8 wt.% to 37.2 wt.%. The latter is in line with the enhanced formation of viscous phase at this temperature interval for RV.

Contrary to R and RV, the mineralogical assemblage for RB is typical of a calcium-rich clay-based ceramic. At 900 °C, åkermanite $CaMgSi_2O_7$ starts to form after the dissociation of calcite, dolomite and the dehydroxylation of clay minerals. The other phases that make up the mineralogical composition of RB are the same with those for R and RV. Nonetheless, compared to R and RV, RB exhibits the highest amount of amorphous phase at 900 °C, 22.7 wt.%. For firing at 950 and 1000 °C, quartz,

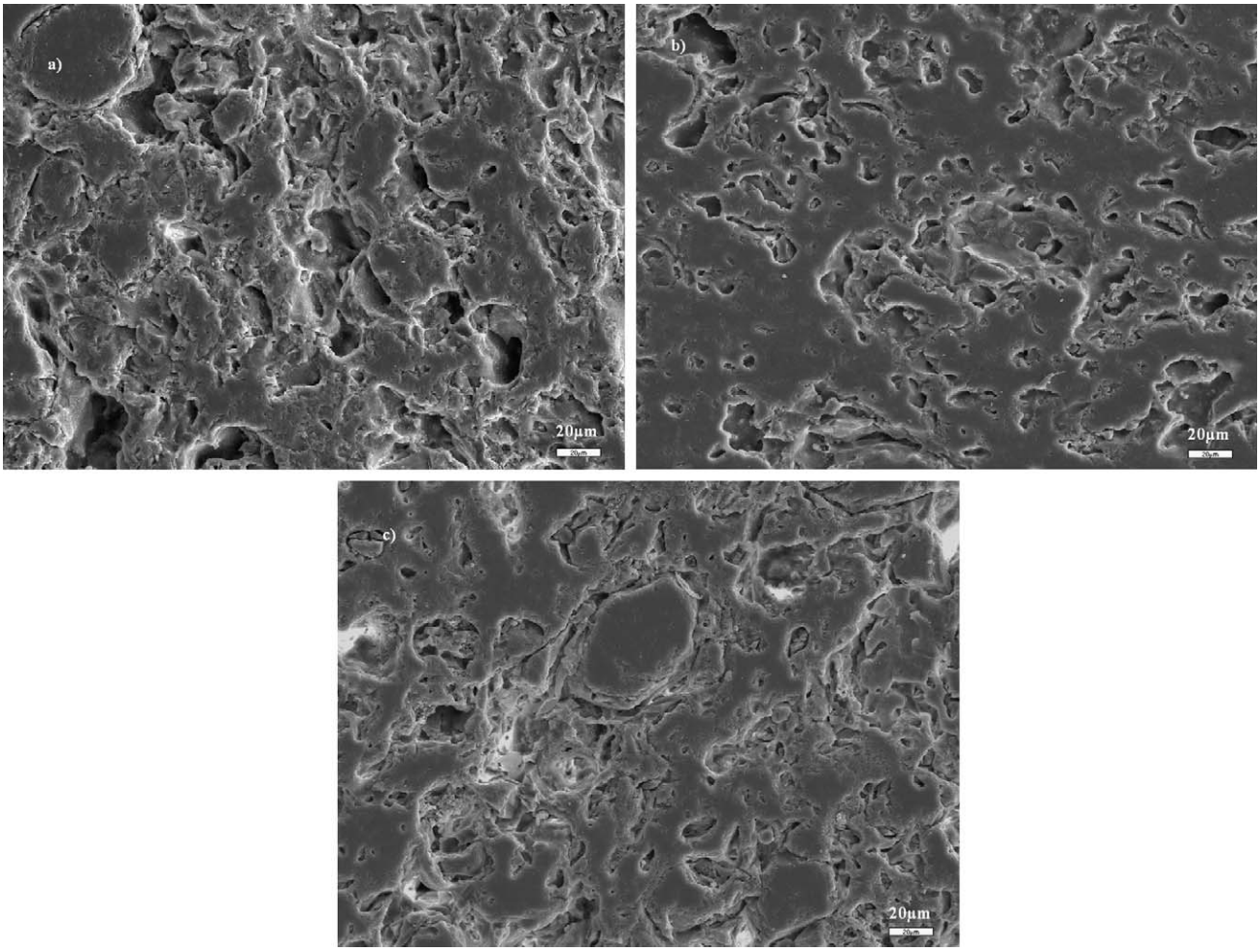

Fig. 10. Secondary electrons' images of polished surface of (a) R, (b) RB and (c) RV, fired at 1000 °C.

albite and sanidine decrease, åkermanite and the amorphous phase increase whereas mica is no longer present. At 1000 °C, quartz is 45.5 wt.%, åkermanite has risen to 4.8 wt.% and the amorphous phase, 28.7 wt.%, is higher than the amorphous content of R (26.4 wt.%) and lower than the amorphous content of RV (37.2 wt.%) (Fig. 7).

Elemental mapping by EDS, carried out on RB2 between the bulk and the surface of the body, Fig. 8, revealed that both boron and sodium are present in higher concentration close to the surface. This is attributed to the migration of water soluble $Na_2B_4O_7$, as already discussed in Section 3.2.

For 900 °C, the secondary electrons' images of all samples tested, Fig. 9, present a similar microstructure, typical for heavy clay bodies, with predominantly open and interconnected porosity and clearly distinguished quartz grains. No notable differences are observed among R, RB and RV. At higher temperatures, 1000 °C, the microstructure is different for each composition, Fig. 10(a–c). The reference sample R has both open and closed pores and vitrification has taken place. RB and RV on the other hand, appear less porous with a higher percentage of closed pores. The formation of glassy phase is enhanced compared to R and a continuous vitrified matrix has been developed. Quartz grains are rounded in shape whereas the smaller ones along with grains of feldspars are embedded in the vitrified areas. The above observations are in line with the measurements on the firing behaviour as well as the physico-mechanical properties.

4. Conclusions

The conclusions of this work can be summarised as follows:

- Addition of 3 wt.% SBW in a clay-based body suitable for the production of red roofing tiles (mixture RB) is compatible with the established ceramic processing followed and did not result in surface migration of boron-containing compounds with adverse effects.
- R and RB demonstrate a comparable dilatometric behaviour and have similar overall shrinkage during firing. In the case of RV, densification initiated 50 °C approximately lower compared to R and RB.
- Both RB and RV presented higher development of liquid phase during firing. For all firing temperatures tested no deformation of the samples was observed.
- Addition of borates resulted in the formation of new crystalline phases. In the case of RB, åkermanite is formed for firing at 900 °C and above, whereas in RV, hercynite for firing at 900 °C and above, and mullite, for firing at 1000 °C. Quantitatively, the differences are small at 900 °C and become noticeable at 1000 °C, especially for RV that demonstrates substantial reduction of quartz and increase of amorphous phase.
- For firing at 1000 °C, the role of borates is intensified. Water absorption is reduced by 16.1% and 18.0%, whereas bending strength increased by 27.6% and 40.8%, for RB and RV respectively, compared to the reference formulation.
- The results are promising for the utilisation of boron waste as a flux in the heavy clay industry.

Acknowledgements

The authors acknowledge the support obtained within the framework of Erasmus and Turkish-Greek bilateral project 05TUR-046 GGET, 105M087 TUBITAK. Etibor Co. Kirka Borax plant, of Eti Maden Works, is also gratefully acknowledged for providing the boron samples.

References

[1] Y. Kar, N. Şen, A. Demirbas, Boron minerals in Turkey, their application areas and importance for the Country's Economy, Minerals & Energy 20 (3–4) (2006) 2–10.
[2] P.M. Mobbs, The Mineral Industry of Turkey. U.S. Geological Survey Minerals Yearbook, Vol III, Africa and Middle East, 2004.
[3] U.S. Geological Survey, Mineral Commodity Summaries, January 2009.
[4] R.A. Smith, Basic geology and chemistry of borate, American Ceramic Society Bulletin 81 (8) (2002) 61–64.
[5] Institute for Prospective Technological Studies, Joint Research Centre Reference Document on Best Available Techniques for Management of Tailings and Waste-Rock in Mining Activities, Sustainability in Industry, Energy and Transport, European IPPC Bureau, European Commission, 2004.
[6] T. Uslu, A.I. Arol, Use of boron waste as an additive in red bricks, Waste Management 24 (2) (2004) 217–220.
[7] T. Kavas, Use of boron waste as a fluxing agent in production of red mud brick, Building and Environment 41 (12) (2006) 1779–1783.
[8] S. Kurama, A. Kara, H. Kurama, The effect of boron waste in phase and microstructural development of a terracotta body during firing, Journal of the European Ceramic Society 26 (4–5) (2006) 755–760.
[9] S. Kurama, A. Kara, H. Kurama, Investigation of borax waste behaviour in tile production, Journal of the European Ceramic Society 27 (2–3) (2007) 1715–1720.
[10] Y. Elbeyli, Y. Kalpakli, J. Gülen, M. Piskin, M. Piskin, Utilization of borax waste as an additive in building brick production, in: Proceedings of the Uluslararasi Bor Sempozyumu, Eskisehir, Turkey, 23–25 September, (2004), pp. 431–436.
[11] A. Olgun, Y. Erdogan, Y. Ayhan, B. Zeybek, Development of ceramic tiles from coal fly ash and tincal ore waste, Ceramics International 31 (1) (2005) 153–158.
[12] A. Christogerou, T. Kavas, Y. Pontikes, S. Koyas, Y. Tabak, G.N. Angelopoulos, Use of boron wastes in the production of heavy clay ceramics, Ceramics International 35 (1) (2009) 447–452.
[13] M. Austerberry and A. Stubbs, Using Borates in Brick and Roofing Tile. In Ceramic Industry 154, No.5, 2004 May, pp 31–37.
[14] A.J. Stubbs, M. Evans, United States Patent Application 20,050,170,945 (2002).
[15] C.R. Ward, J.C. Taylor, C.E. Matulis, L.S. Dale, Quantification of mineral matter in the Argonne Premium coals using interactive Rietveld-based X-ray diffraction, International Journal of Coal Geology 46 (2–4) (2001) 67–82.
[16] Standard Test Method ISO 10545-3, Ceramic Tiles—Part 3: Determination of Water Absorption, Apparent Porosity, Apparent Relative Density and Bulk Density, 1995.
[17] T. Peters, R. Iberg, Mineralogical changes during firing of calcium-rich brick clays, American Ceramic Society Bulletin 57 (1978) 503–509.
[18] E.D. Garrett, Borates, Handbook of Deposits, Processing Properties and Use, Academic Press, 1998.
[19] T. Kavas, A. Christogerou, Y. Pontikes, N. Sönmez, G.N. Angelopoulos, Production of lightweight aggregates from different types of boron wastes, in: Proceedings of the 7th Ceramic Congress, Afyon Karahisar, Turkey, 2008.

[20] A. Ekmekyapar, A. Baysar, A. Künkül, Dehydration kinetics of tincal and borax by thermal analysis, Industrial and Engineering Chemistry Research 36 (9) (1997) 3487–3490.
[21] I. Waclawska, Thermal decomposition of borax, Journal of Thermal Analysis 43 (1) (1995) 261–269.
[22] S. Gunasekaran, G. Anbalagan, Thermal decomposition of natural dolomite, Bulletin of Materials Science 30 (4) (2007) 339–344.
[23] L. Maritan, L. Nodari, C. Mazzoli, A. Milano, U. Russo, Influence of firing conditions on ceramic products: experimental study on clay rich in organic matter, Applied Clay Science 31 (1–2) (2006) 1–15.
[24] G. Cultrone, C. Rodriguez-Navarro, E. Sebastian, O. Cazalla, M.J. De La Torre, Carbonate and silicate phase reactions during ceramic firing, European Journal of Mineralogy 13 (3) (2001) 621–634.